

Reactions of Cyclometalated Oxazoline Half-Sandwich Complexes of Iridium and Ruthenium with Alkynes and CO

David L. Davies,* Omar Al-Duaij, John Fawcett, and Kuldeep Singh

Department of Chemistry, University of Leicester, Leicester, LE1 7RH U.K.

Received December 18, 2009

The ligand 4,4-dimethyl-2-oxazolinybenzene is easily cyclometalated by $[\text{IrCl}_2\text{Cp}^*]_2$ or $[\text{RuCl}(\text{MeCN})_2(p\text{-cymene})\text{PF}_6]$ in the presence of sodium acetate. In the case of iridium the resultant complex dissolves in acetonitrile in the presence of KPF_6 to give an acetonitrile-coordinated cationic complex. The analogous complex is formed directly in the ruthenium cyclometalation reaction. These labile cationic complexes undergo insertion reactions with internal and terminal alkynes. Internal alkynes give only monoinsertion products, whereas terminal alkynes give mono- or di-insertion products. The cations will also react with CO, but no insertion occurs in this case.

Introduction

Cyclometalated complexes have been known for a long time and have proven to be useful in organic synthesis and as catalysts or catalyst precursors.¹ However, much of the early work involved the use of stoichiometric amounts of the transition metal or required halogenated precursors to form the M–C bond, neither of which is desirable from a financial or atom-economic perspective. In recent years there has been substantial progress in catalytic C–H bond activation and subsequent C–C bond formation, which potentially provides a much cheaper and atom-economic methodology.² One of the most general strategies involves regioselective C–H functionalization dependent on coordination of an adjacent functional group; metalation of an ortho C–H bond of a substituted phenyl to form a five-membered ring is particularly common. Coupling a C–H bond activation step with an alkyne insertion into the cyclometalated M–C bond and subsequent reductive elimination is a potential route to heterocyclic products (Scheme 1). In this regard studies of the stoichiometric reactions of cyclometalated

complexes with alkynes are important to understand selectivity and reactivity issues in the catalytic processes.

Stoichiometric reactions of alkynes with cyclopalladated complexes have been widely studied and have found application in the synthesis of heterocyclic molecules.^{3–5} The reactivity of half-sandwich cyclometalated complexes with unsaturated substrates is, however, comparatively little studied, possibly due to a lack of general routes to such complexes (see below). Early work by Pfeffer et al. showed that arene ruthenium cyclometalated complexes $[\text{RuCl}(\text{DMBA})(\text{arene})]$ (DMBAH = dimethylbenzylamine) would react with alkynes to form coordinated isoquinolinium salts, which could be liberated from the metal using copper salts as oxidants.^{6–8} Recently Jones et al. have shown that related Cp^*Rh and Cp^*Ir cyclometalated phenylpyridine complexes undergo alkyne insertion and generate isoquinolinium salts at room temperature after oxidative coupling with CuCl_2 .⁹ Miura and co-workers have recently reported a number of catalytic reactions to form heterocycles in which they propose that cyclometalation at Cp^*Rh followed by alkyne insertion into the M–C bond are important steps in the catalytic cycle.¹⁰ A similar sequence is likely involved in

*Corresponding author. E-mail: dld3@le.ac.uk.

(1) For general reviews of cyclometalated complexes see: (a) Pfeffer, M. *Pure Appl. Chem.* **1992**, *64*, 335. (b) Omae, I. *Coord. Chem. Rev.* **2004**, *248*, 995. For cyclopalladated complexes see for example: (c) Ryabov, A. D. *Synthesis* **1985**, 233. (d) Dupont, J.; Pfeffer, M.; Spencer, J. *Eur. J. Inorg. Chem.* **2001**, 1917. (e) Bedford, R. B. *Chem. Commun.* **2003**, 1787. (f) Dupont, J.; Consorti, C. S.; Spencer, J. *Chem. Rev.* **2005**, *105*, 2527. For a recent review of cycloruthenated complexes see: (g) Djukic, J. P.; Sortais, J. B.; Barloy, L.; Pfeffer, M. *Eur. J. Inorg. Chem.* **2009**, 817.

(2) (a) Alberico, D.; Scott, M. E.; Lautens, M. *Chem. Rev.* **2007**, *107*, 174. (b) Kakiuchi, F.; Kochi, T. *Synthesis* **2008**, 3013. (c) Lewis, J. C.; Bergman, R. G.; Ellman, J. A. *Acc. Chem. Res.* **2008**, *41*, 1013. (d) Satoh, T.; Miura, M. *Chem. Lett.* **2007**, *36*, 200. (e) Dyker, G., Ed. *Handbook of C-H Transformations*; Wiley-VCH: Weinheim, 2005.

(3) (a) Spencer, J.; Pfeffer, M.; Decian, A.; Fischer, J. *J. Org. Chem.* **1995**, *60*, 1005. (b) Maassarani, F.; Pfeffer, M.; Spencer, J.; Wehman, E. *J. Organomet. Chem.* **1994**, *466*, 265. (c) Beydoun, N.; Pfeffer, M.; Decian, A.; Fischer, J. *Organometallics* **1991**, *10*, 3693. (d) Wu, G.; Rheingold, A. L.; Geib, S. J.; Heck, R. F. *Organometallics* **1987**, *6*, 1941. (e) Wu, G. Z.; Rheingold, A. L.; Heck, R. F. *Organometallics* **1986**, *5*, 1922. (f) Wu, G. Z.; Geib, S. J.; Rheingold, A. L.; Heck, R. F. *J. Org. Chem.* **1988**, *53*, 3238.

(4) Spencer, J.; Pfeffer, M.; Kyritsakas, N.; Fischer, J. *Organometallics* **1995**, *14*, 2214.

(5) Maassarani, F.; Pfeffer, M.; Leborgne, G. *Organometallics* **1987**, *6*, 2029.

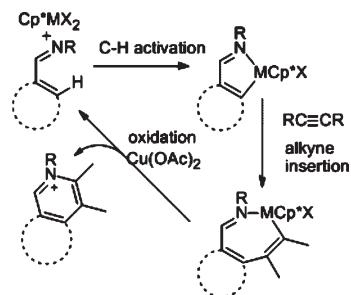
(6) Pfeffer, M.; Sutter, J. P.; Urriolabeitia, E. P. *Bull. Soc. Chim. Fr.* **1997**, *134*, 947.

(7) Abbenhuis, H. C. L.; Pfeffer, M.; Sutter, J.-P.; de Cian, A.; Fischer, J.; Ji, H. L.; Nelson, J. H. *Organometallics* **1993**, *12*, 4464.

(8) Ferstl, W.; Sakodinskaya, I. K.; Beydoun-Sutter, N.; LeBorgne, G.; Pfeffer, M.; Ryabov, A. D. *Organometallics* **1997**, *16*, 411.

(9) Li, L.; Brennessel, W. W.; Jones, W. D. *J. Am. Chem. Soc.* **2008**, *130*, 12414.

(10) (a) Fukutani, T.; Umeda, N.; Hirano, K.; Satoh, T.; Miura, M. *Chem. Commun.* **2009**, 5141. (b) Kokubo, K.; Matsumasa, K.; Nishinaka, Y.; Miura, M.; Nomura, M. *Bull. Chem. Soc. Jpn.* **1999**, *72*, 303. (c) Mochida, S.; Hirano, K.; Satoh, T.; Miura, M. *J. Org. Chem.* **2009**, *74*, 6295. (d) Shimizu, M.; Hirano, K.; Satoh, T.; Miura, M. *J. Org. Chem.* **2009**, *74*, 3478. (e) Shimizu, M.; Tsurugi, H.; Satoh, T.; Miura, M. *Chem. – Asian J.* **2008**, *3*, 881. (f) Ueura, K.; Satoh, T.; Miura, M. *Org. Lett.* **2007**, *9*, 1407. (g) Ueura, K.; Satoh, T.; Miura, M. *J. Org. Chem.* **2007**, *72*, 5362. (h) Umeda, N.; Tsurugi, H.; Satoh, T.; Miura, M. *Angew. Chem., Int. Ed.* **2008**, *47*, 4019.

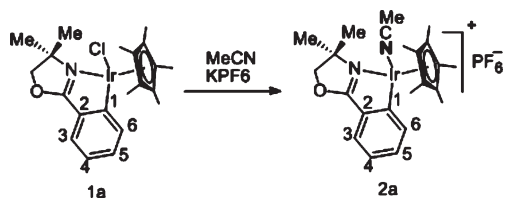
Scheme 1. Possible Catalytic Cycle for the Production of Heterocycles via C–H Activation and Alkyne Insertion


Cp*Rh-catalyzed synthesis of indoles¹¹ and isoquinolines¹² reported by Fagnou. In the latter case Fagnou provided evidence to suggest that, in some cases at least, C–N reductive elimination can occur before oxidation by copper salts.¹²

In 2003 we reported a new route to half-sandwich (Cp*M, M = Rh, Ir, or {*p*-cymene}Ru) cyclometalated complexes via an acetate-assisted C–H activation.¹³ Subsequent studies by us¹⁴ and others¹⁵ have shown that these are ambiphilic metal ligand activations (AMLA),¹⁶ involving an electrophilic metal center with assistance by hydrogen bonding to the free arm of a coordinated acetate. Having discovered a facile high-yield route to a range of half-sandwich cyclometalated complexes, we now disclose some of our results on the reactivity of cyclometalated oxazolines with alkynes that are relevant to the catalytic formation of heterocycles reported by Miura¹⁰ and Fagnou.^{11,12}

Results and Discussion

Complex **1a** was reacted with PhC≡CPh in MeCN in the presence of excess KPF₆. Monitoring the reaction by electro-spray mass spectrometry showed that even after 72 h the reaction had not gone to completion. It is possible that MeCN competes with PhC≡CPh to replace the chloride in **1a**. The reaction is considerably slower than alkyne insertions observed by Pfeffer^{6,7} and Jones⁹ for related species when the reactions were conducted in methanol. It is known that alkyne insertions into cyclopalladated complexes are more efficient if the initial complex is cationic.⁵ Hence we prepared the cationic MeCN complex **2a** by reaction of **1a** with KPF₆.



(11) Stuart, D. R.; Bertrand-Laperle, M.; Burgess, K. M. N.; Fagnou, K. *J. Am. Chem. Soc.* **2008**, *130*, 16474.

(12) Guimond, N.; Fagnou, K. *J. Am. Chem. Soc.* **2009**, *131*, 12050.

(13) Davies, D. L.; Al-Duaij, O.; Fawcett, J.; Giardiello, M.; Hilton, S. T.; Russell, D. R. *Dalton Trans.* **2003**, 4132.

(14) (a) Davies, D. L.; Donald, S. M. A.; Al-Duaij, O.; Macgregor, S. A.; Polleth, M. *J. Am. Chem. Soc.* **2006**, *128*, 4210. (b) Boutadla, Y.; Davies, D. L.; Macgregor, S. A.; Poblador-Bahamonde, A. I. *Dalton Trans.* **2009**, 5887.

(15) Li, L.; Brennessel, W. W.; Jones, W. D. *Organometallics* **2009**, *28*, 3492.

(16) Boutadla, Y.; Davies, D. L.; Macgregor, S. A.; Poblador-Bahamonde, A. I. *Dalton Trans.* **2009**, 5820.

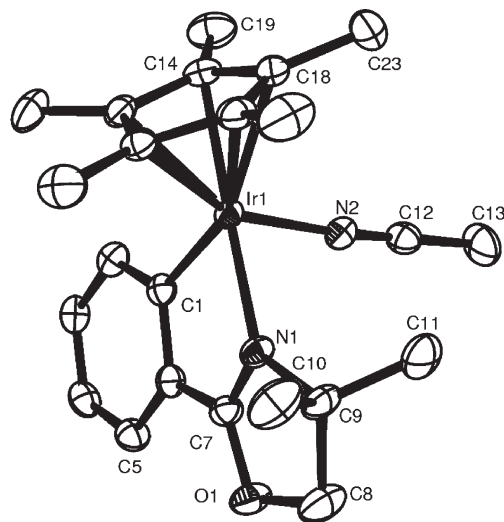


Figure 1. Molecular structure and atom-numbering scheme for the cation of **2a** with 50% displacement ellipsoids. All H atoms are omitted for clarity. Selected bond distances (Å) and angles (deg): Ir–N(1) 2.118(3), Ir–N(2) 2.050(3), Ir–C(1) 2.068(3), Ir–C(14) 2.153(3), Ir–C(15) 2.173(3), Ir–C(16) 2.167(4), Ir–C(17) 2.170(3), Ir–C(18) 2.240(3), Ir–C(22) 2.168(6), C(1)–Ir–N(1) 77.08(12), C(1)–Ir–N(2) 88.62(12), N(1)–Ir–N(2) 82.85(11).

The ¹H NMR spectrum of **2a** shows four multiplets in the aromatic region as expected; however, the oxazoline methyls give rise to a broad singlet at δ 1.47, while the CH₂ protons are observed as a sharp singlet at δ 4.58 and coordinated NCMe gives a broad singlet at δ 2.42, 0.42 ppm downfield from free NCMe. The equivalence of the CMe₂ and of the CH₂ protons suggests that the complex is fluxional on the NMR time scale via dissociation of MeCN accompanied by epimerization at the metal center; such a process has been observed previously for [Ru(MeCN)(DMBA)(arene)]⁺.¹⁷ The ¹H NMR spectrum at 273 K showed two sharp singlets at δ 1.44 and 1.54 for the CMe₂ protons and the broad singlet due to NCMe resolved into two singlets at δ 2.42 (coordinated NCMe) and 2.02 (free NCMe) (10:1 ratio), the latter observation consistent with exchange of free and coordinated NCMe being slow at this temperature. Further cooling to 233 K led to resolution of the CH₂ signal to two mutually coupled doublets at δ 4.40 and 4.70; hence, at this temperature epimerization is slow compared to the NMR time scale.

The structure of **2a** has been determined by X-ray crystallography and is shown in Figure 1, with selected bond distances and angles. The complex adopts the expected pseudo-octahedral structure and confirms the coordination of NCMe. The chelate bite angle C(1)–Ir(1)–N(1) [77.08(12)°] is similar to that [78.0(2)°] in the related [IrCl(Phpy)Cp*]⁺^{9,18} (PhpyH = 2-phenylpyridine). The M–N(1) bond length [2.118(3) Å] is longer than M–N(2) [2.050(3) Å], consistent with a bond to an sp² rather than an sp-hybridized nitrogen. As found for other cyclometalated Cp*Rh/Ir complexes, the Cp* is bonded in an asymmetric fashion with three shorter Ir–C distances (ca. 2.16 Å) and two longer Ir–C distances (ca. 2.25 Å).^{13,18,19}

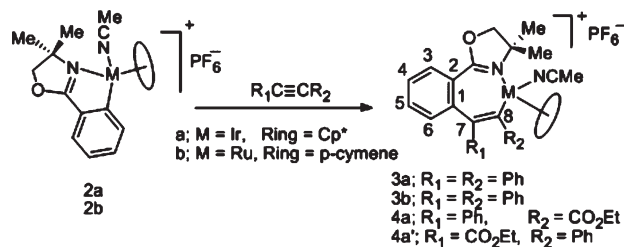
(17) Robitzner, M.; Rittleng, V.; Sirlin, C.; Dedieu, A.; Pfeffer, M. *C. R. Chim.* **2002**, *5*, 467.

(18) Boutadla, Y.; Al-Duaij, O.; Davies, D. L.; Griffith, G. A.; Singh, K. *Organometallics* **2009**, *28*, 433.

(19) Scheeren, C.; Maasarani, F.; Hijazi, A.; Djukic, J. P.; Pfeffer, M.; Zaric, S. D.; LeGoff, X. F.; Ricard, L. *Organometallics* **2007**, *26*, 3336.

We have previously reported that acetate-assisted cyclometalation of oxazolines with $[\text{RuCl}_2(p\text{-cymene})]_2$ failed.¹³ However, we can now report that if the reaction is carried out in acetonitrile at 45 °C starting from $[\text{RuCl}(\text{MeCN})_2(p\text{-cymene})][\text{PF}_6]$, then the reaction works, providing acetonitrile complex **2b**. This process is similar to that used previously by Pfeffer et al. for cyclometalation of benzylamines except that NaOH was used as base in those cases.²⁰ The ¹H NMR spectrum of **2b** shows appropriate signals for the cyclometalated oxazoline, namely, four multiplets in the aromatic region, two singlets at δ 1.47 and 1.57 due to the methyls, and a singlet for the CH₂ protons, which are accidentally equivalent, at δ 4.50. The *p*-cymene shows the expected signals for a chiral complex, and the coordinated NCMe gives a broad singlet at δ 2.21, 0.2 ppm downfield from free NCMe. The inequivalence of the oxazoline methyls and of the *p*-cymene protons suggests that, unlike **2a** discussed above, the rate of epimerization of **2b** is slow on the NMR time scale. It is known that ligand substitution is much slower for arene ruthenium complexes than the corresponding Cp*Ir ones.²¹

Having prepared cationic cyclometalated species **2a,b**, containing labile MeCN ligands, these complexes were then reacted with alkynes. Reaction of **2a** with PhC≡CPh occurred within a few hours at room temperature in dichloromethane to give monoinsertion product **3a**. The ¹H NMR spectrum of **3a** shows signals due to the Cp*, the oxazoline ligand, and PhC≡CPh in a 1:1:1 ratio. The CMe₂ group gives rise to two singlets at δ 1.31 and 1.37; the CH₂ protons are also inequivalent, giving two mutually coupled doublets at δ 4.27 and 4.58. The inequivalence of the CH₂ protons and the methyls of the CMe₂ group is consistent with the metal center being chiral and shows that epimerization at the metal is slow on the NMR time scale. A singlet integrating to 3H at δ 2.00 is assigned to NCMe protons. This signal and that for the Cp* are both upfield (0.42 and 0.48 ppm, respectively) of the corresponding signals in **2a**, suggesting they are affected by the presence of ring currents. The NOESY spectrum shows cross-peaks between the signals for Cp* and the doublets for H³ and H⁶, confirming that the Cp* lies over the original cyclometalated phenyl (see X-ray structure of **3b** below). Similar upfield shifts of Cp* resonances have been observed for benzene bis(oxazoline) complexes, which have a similar seven-membered chelate ring.²²



The ¹³C{¹H} NMR spectrum shows the expected signals with the original cyclometalated carbon now being observed at ca. δ 146, about 33 ppm upfield compared with **2a**, a large shift, consistent with insertion of alkyne into the M–C bond,

(20) Fernandez, S.; Pfeffer, M.; Rittler, V.; Sirlin, C. *Organometallics* **1999**, *18*, 2390.

(21) Dacsi, L.; Elias, H.; Frey, U.; Hornig, A.; Koelle, U.; Merbach, A. E.; Paulus, H.; Schneider, J. S. *Inorg. Chem.* **1995**, *34*, 306.

(22) Davies, D. L.; Fawcett, J.; Garratt, S. A.; Russell, D. R. *Organometallics* **2001**, *20*, 3029.

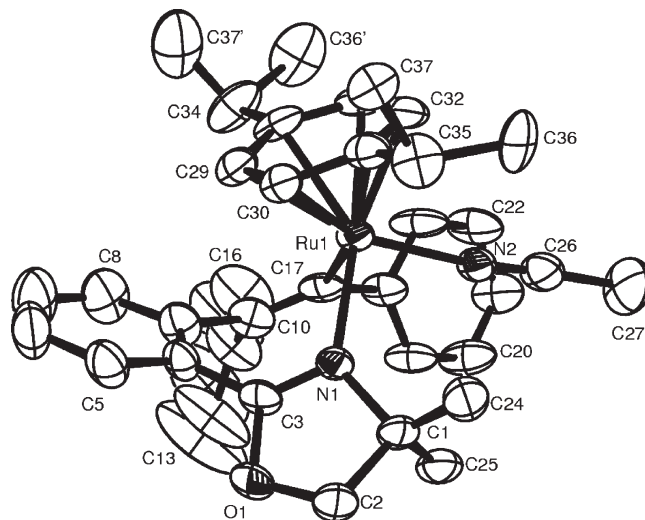


Figure 2. Molecular structure and atom-numbering scheme for the cation of **3b** with 50% displacement ellipsoids. All H atoms are omitted for clarity. The ¹Pr and Me groups of the *p*-cymene are disordered. Selected bond distances (Å) and angles (deg): Ru–C(17) 2.095(4), Ru–N(1) 2.123(3), Ru–N(2) 2.053(3), C(17)–C(10) 1.336(6); C(17)–Ru–N(1) 81.50(13), C(17)–Ru–N(2) 88.73(16), N(1)–Ru–N(2) 89.80(13).

as found by Pfeffer,⁷ not into the M–N bond.²³ The FAB mass spectrum of **3a** shows an ion at m/z 679 due to $[\text{M} - \text{NCMe}]^+$, confirming the presence of PhC≡CPh.

Ruthenium complex **3b** was obtained similarly from the reaction of **2b** with PhC≡CPh in CH₂Cl₂ but required a longer reaction time (24 h), consistent with the slower rate of substitution at arene ruthenium compared with Cp*Ir.²¹ The ¹H NMR spectrum of the crude product showed more than one Ru(*p*-cymene) complex; however, after filtration through silica only one product, **3b**, remained. The ¹H NMR spectrum of **3b** is similar to that of **3a** with signals for the *p*-cymene replacing the Cp*. As found in **3a**, the NCMe protons in **3b** are strongly shielded at δ 1.78, 0.43 ppm upfield from **2b**; the four multiplets of the *p*-cymene are also shifted 0.5–0.8 ppm upfield from **2b**. The CMe₂ group gives rise to two singlets at δ 1.09 and 1.59, and the CH₂ protons are also inequivalent, giving two mutually coupled doublets at δ 4.34 and 4.47. These observations confirm that epimerization at the metal is slow on the NMR time scale.

Recrystallization from dichloromethane/hexane gave X-ray quality crystals of **3b**. The crystal structure is shown in Figure 2, with selected bond distances and angles. The complex adopts the expected pseudo-octahedral structure and confirms that the alkyne has, as expected, inserted into the M–C bond rather than the M–N bond,²³ with formation of a seven-membered ring. The C(17)–Ru(1)–N(1) chelate bite angle of the seven-membered ring [81.50(13)°] is larger than that [77.08(12)°] in the five-membered ring of **2a**. The oxazoline ring is rotated out of the plane of the phenyl [C(4)–C(9)] with a dihedral angle [N(1)–C(3)–C(4)–C(9)] of 52.8°, which is much larger than the corresponding angle (4.5°) in **2a**. Presumably, this occurs as a consequence of the expansion in ring size. Similar tilting of the oxazoline ring is seen in benzene bisoxazoline complexes with a seven-membered ring.²² The structure also shows that

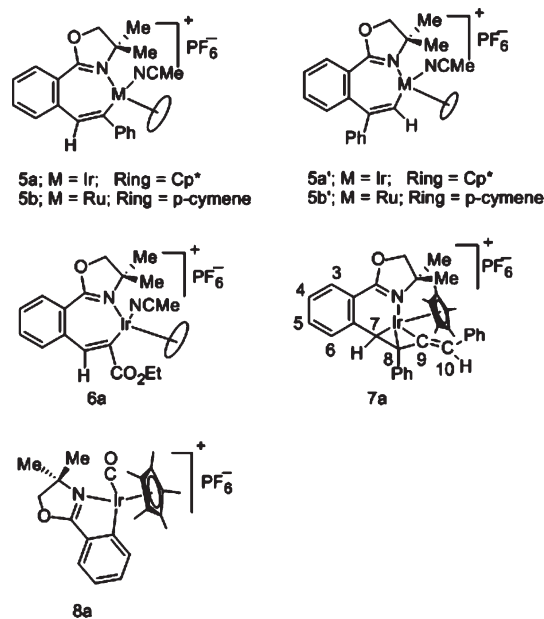
(23) Cabeza, J. A.; del Rio, I.; Grepioni, F.; Moreno, M.; Riera, V.; Suarez, M. *Organometallics* **2001**, *20*, 4190.

the NCMe lies in the region of the ring current of the phenyl [C(18)–C(23)] and the *p*-cymene is tilted to lie over the ring [C(4)–C(9)]. These features account for the high-field shifts observed in the ^1H NMR spectrum of **3b** (see above). Similar features are expected for **3a**.

To assess the regioselectivity of the alkyne insertion, reaction of **2a** with $\text{PhC}\equiv\text{CCO}_2\text{Et}$ was investigated. The ^1H NMR spectrum of the crude product showed only one species. A singlet at δ 2.77 assigned to a coordinated NCMe is at much lower field than in **3a** (δ 2.00), suggesting that it is not affected by a ring current of an adjacent phenyl, consistent with phenyl being on the carbon atom adjacent to the phenyl oxazoline, i.e., isomer **4a**. The Cp^* is observed at δ 1.41, 0.4 ppm upfield from **2a**, consistent with a ring-current effect from the originally cyclometalated phenyl. The CMe_2 group gives rise to two sharp singlets at δ 1.31 and 1.46, with the OCH_2 protons being observed as two doublets at δ 4.23 and 4.53; the inequivalence is consistent with epimerization at the metal being slow on the NMR time scale. Two multiplets are observed at δ 1.38 and 3.79, assigned to the CO_2Et protons. The $^{13}\text{C}\{^1\text{H}\}$ NMR spectrum shows the expected number of carbon signals, and the FAB mass spectrum shows an ion at m/z 676 due to $[\text{M} - \text{NCMe}]^+$. The IR spectrum shows $\nu(\text{C}=\text{N})$ at 1624 cm^{-1} , similar to that in the starting cationic complex with $\nu(\text{C}=\text{O})$ at 1695 cm^{-1} , confirming the presence of $\text{PhC}\equiv\text{CCO}_2\text{Et}$. The spectroscopic data are consistent with isomer **4a**; that is, the insertion occurs such that the ester group is found on the carbon atom adjacent to the metal, with the phenyl group being on the carbon atom adjacent to the phenyl oxazoline. The regioselectivity is the same as that found by Pfeffer for reaction of this alkyne with $[\text{RuCl}(\text{DMBA})(\text{C}_6\text{H}_6)]$,⁶ which is opposite that usually observed for insertion into the M–C bond of palladium complexes^{4,5,24} and nickel complexes.²⁵ The regioselectivity of insertion of this alkyne has also been studied experimentally and computationally, and the regioselectivity was found to depend on the exact palladium precursor used; more electrophilic palladium species, particularly cationic ones, favored insertion with the ester next to the metal.²⁶

It is notable that in most studies involving catalytic reactions of alkynes with cyclometalated intermediates there are relatively few examples that involve terminal alkynes,²⁷ and the first example in which the cyclometalated intermediate is generated by C–H activation was only reported in 2008.²⁸ This may be due to the greater reactivity of terminal alkynes leading to polymerization reactions and/or the possibility of forming vinylidene complexes. Similarly to our knowledge the only example of a stoichiometric reaction of a half-sandwich cyclometalated complex with a terminal alkyne is that of $[\text{CoI}(\text{DMBA})(\text{Cp})]$,²⁹ which reacts only with terminal alkynes. Hence, we thought it would be informative to test the reaction of **2a,b** with $\text{PhC}\equiv\text{CH}$.

In the course of our preliminary studies of the reaction of $\text{PhC}\equiv\text{CH}$ with the chloride complex **1a** even when only one equivalent of alkyne was used, the ES mass spectrum often showed ions due to a mixture of products corresponding to insertion of one or two equivalents of alkyne, suggesting that insertion of a second molecule of $\text{PhC}\equiv\text{CH}$ occurred at a similar rate to the first insertion. To try to overcome these difficulties, we again started from the acetonitrile complex **2a**. Reaction of $\text{PhC}\equiv\text{CH}$ with **2a** in 1:1 ratio in CH_2Cl_2 led to formation of a monoinsertion complex, **5a**, in 86% yield after 1 h. The ^1H NMR spectrum of the product showed only one isomer was present. The signal for the coordinated NCMe was observed at δ 1.99, more than 0.4 ppm upfield from the corresponding signal in **2a**, consistent with a ring current from an adjacent phenyl, as discussed previously for **3a**. This suggests that the phenyl of $\text{PhC}\equiv\text{CH}$ is adjacent to iridium and the product is **5a** rather than **5a'** (confirmed by X-ray crystallography; see below). Unfortunately the signal for the alkyne proton is underneath signals for the alkyne phenyl, so NOE effects could not be used to corroborate the assignment of which regioisomer was formed. The CMe_2 group gave two singlets at δ 1.14 and 1.29, and the OCH_2 protons were observed as two mutually coupled doublets at δ 4.11 and 4.42. The inequivalence of the CH_2 protons and of the methyls of the CMe_2 group is consistent with the chiral center at the metal and that epimerization at the metal is slow on the NMR time scale. The $^{13}\text{C}\{^1\text{H}\}$ NMR spectrum of **5a** shows the expected signals. FAB mass spectrometry showed only a peak at m/z 602 $[\text{M} - \text{NCMe}]^+$ corresponding to monoininsertion of $\text{PhC}\equiv\text{CH}$.



(24) Pfeffer, M.; Rottevel, M. A.; Le Borgne, G.; Fischer, J. *J. Org. Chem.* **2002**, *57*, 2147.

(25) (a) Bennett, M. A.; Macgregor, S. A.; Wenger, E. *Helv. Chim. Acta* **2001**, *84*, 3084. (b) Edwards, A. J.; Macgregor, S. A.; Rae, A. D.; Wenger, E.; Willis, A. C. *Organometallics* **2001**, *20*, 2864.

(26) Kelly, A. E.; Macgregor, S. A.; Willis, A. C.; Nelson, J. H.; Wenger, E. *Inorg. Chim. Acta* **2003**, *352*, 79.

(27) (a) Korivi, R. P.; Cheng, C.-H. *Org. Lett.* **2005**, *7*, 5179.

(b) Korivi, R. P.; Wu, Y.-C.; Cheng, C.-H. *Chem.—Eur. J.* **2009**, *15*, 10727.

(28) Chuan-Che, L.; Rajendra Prasad, K.; Chien-Hong, C. *Chem.—Eur. J.* **2008**, *14*, 9503.

(29) Meneghetti, M. R.; Grellier, M.; Pfeffer, M.; Fischer, J. *Organometallics* **2000**, *19*, 1935.

The corresponding reaction was also attempted with the cycloruthenated complex **2b**. The ^1H NMR spectrum of the crude product showed a mixture of species; however after filtration through silica only one product was isolated. The ^1H NMR spectrum is similar to that of **5a** but with signals due to the *p*-cymene in place of the Cp^* . Notably the signal for coordinated NCMe is observed at δ 1.85, 0.36 ppm upfield from that in **2b**, consistent with the phenyl of the alkyne being next to ruthenium, and the product is **5b** not **5b'**. Unfortunately, as for **5a**, due to the overlap of signals NOE effects could not be used to corroborate the assignment of

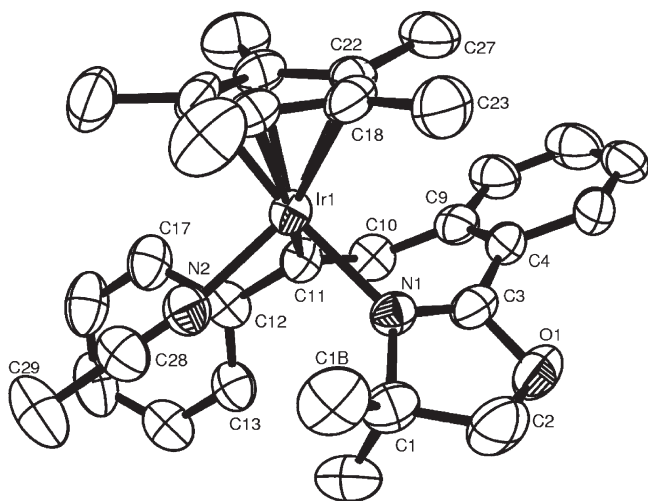


Figure 3. Molecular structure and atom-numbering scheme for the cation of **5a** with 50% displacement ellipsoids. All H atoms are omitted for clarity. Selected bond distances (Å) and angles (deg): Ir–N(1) 2.095(4), Ir–N(2) 2.058(6), Ir–C(11) 2.079(5), Ir–C(18) 2.234(6), Ir–C(19) 2.247(6), Ir–C(20) 2.171(5), Ir–C(21) 2.169(6), Ir–C(22) 2.168(6), C(10)–C(11) 1.331(8); C(11)–Ir–N(1) 81.7(2), C(11)–Ir–N(2) 85.92(9), N(1)–Ir–N(2) 86.3(2).

which regioisomer was formed. The $^{13}\text{C}\{^1\text{H}\}$ NMR spectrum showed the expected signals, and the FAB mass spectrum showed an ion at m/z 512 due to $[\text{M} - \text{NCMe}]^+$, confirming insertion of $\text{PhC}\equiv\text{CH}$.

Careful recrystallization of **5a** and **5b** from dichloromethane/ether gave crystals suitable for X-ray diffraction, and the structures are shown in Figures 3 and 4, respectively, with selected distances and angles. Each complex adopts the expected pseudo-octahedral structure and shows that the alkyne has inserted into the M–C bond to form a seven-membered ring. In both cases the phenyl of the alkyne is on the carbon attached to the metal. The bond lengths and angles are similar in both complexes. In **5b** the Ru–C(11) bond length [2.097(3) Å] and the chelate angle N(1)–Ru(1)–C(11) [83.49(10)°] are similar to the $\text{PhC}\equiv\text{CPh}$ insertion product **3b** [2.095(4) Å and 81.50(13)°, respectively], although the Ru–N(1) bond length [2.094(2) Å] is shorter than that [2.123(3) Å] in **3b**. As found in **3b**, in both **5a** and **5b** the oxazoline is rotated out of the plane of the phenyl C(4)–C(9) (dihedral angle N(1)–C(3)–C(4)–C(9) = 48.4° and 44.5°, respectively). In **5a**, as found in **2a** (see above) the Cp* is bonded in an asymmetric fashion with three shorter Ir–C distances (ca. 2.17 Å) and two longer Ir–C distances (ca. 2.24 Å).^{13,18,19} The structures confirm that the NCMe lies in the region of the ring current of the alkyne phenyl and that the Cp* and *p*-cymene lie over the original cyclometalated phenyl ring.

To investigate possible electronic effects on the regioselectivity of the alkyne insertion, $\text{HC}\equiv\text{CCO}_2\text{Et}$ was also reacted with **2a**. The ^1H NMR spectrum of the reaction mixture showed only one product, **6a**. The ^1H NMR spectrum of **6a** shows the signal for coordinated NCMe protons at δ 2.71, downfield relative to **3a** and **5a** but similar to **4a**, since there is no phenyl substituent on the alkyne. The CMe_2 group shows two sharp singlets at δ 1.22 and 1.37, with the OCH_2 protons observed as two doublets at δ 4.11 and 4.38, the inequivalence consistent with epimerization at the metal being slow

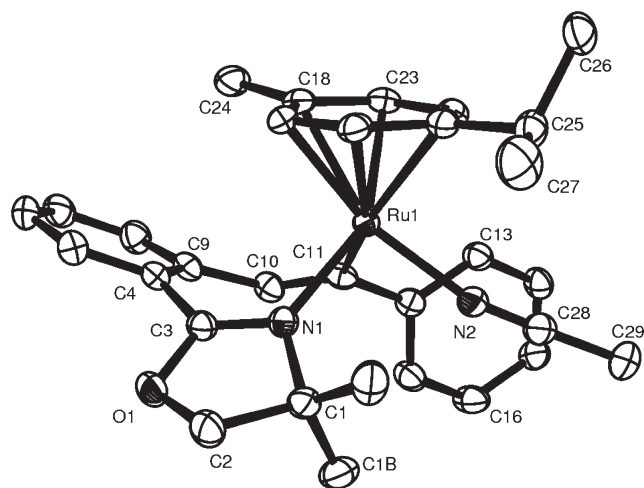


Figure 4. Molecular structure and atom-numbering scheme for the cation of **5b** with 50% displacement ellipsoids. All H atoms are omitted for clarity. Selected bond distances (Å) and angles (deg): Ru–C(11) 2.097(3), Ru–N(1) 2.094(2), Ru–N(2) 2.059(2), C(10)–C(11) 1.347(4); C(11)–Ru–N(1) 83.49(10), C(11)–Ru–N(2) 86.53(7), N(1)–Ru–N(2) 86.14(10).

on the NMR time scale. Two multiplets at δ 1.27 and 4.11 are assigned to the CO_2Et protons, and the original alkyne proton (H^7) is observed as a singlet at δ 7.48. A NOESY spectrum showed that (H^7) is adjacent to (H^6), confirming that the insertion occurs with the CO_2Et ending up on the carbon atom adjacent to the metal. The $^{13}\text{C}\{^1\text{H}\}$ NMR spectrum showed the expected number of carbon signals, and the FAB mass spectrum showed an ion at m/z 600 due to $[\text{M} - \text{NCMe}]^+$. The IR spectrum showed $\nu(\text{C}=\text{N})$ at 1622 cm^{-1} , similar to that in the starting complex **2a**, and $\nu(\text{C}=\text{O})$ at 1682 cm^{-1} , confirming the incorporation of $\text{HC}\equiv\text{CCO}_2\text{Et}$. Pfeffer previously suggested that the regioselectivity of alkyne insertion with $[\text{RuCl}(\text{DMBA})(\text{arene})]$ depends mainly on steric factors.^{6,7} However, the fact that the regioselectivity we observe for $\text{HC}\equiv\text{CCO}_2\text{Et}$ is the same as that for $\text{PhC}\equiv\text{CCO}_2\text{Et}$ suggests that at least in these cases, with an alkyne containing one very electron-withdrawing substituent, electronic factors are also important.

Having observed clean insertion reactions with one equivalent of $\text{PhC}\equiv\text{CH}$, the reaction of **2a** with two equivalents of $\text{PhC}\equiv\text{CH}$ was attempted. Monitoring the reaction by electrospray mass spectrometry suggested that the reaction was complete after two hours. The ^1H NMR spectrum of the product showed a 1:1:2 ratio of the Cp*, oxazoline, and alkyne ligands, as expected for the formation of a di-insertion product. The Cp* signal was observed at δ 1.76, 0.42 ppm downfield compared with the monoinsertion complex **5a**, suggesting it is no longer influenced by a ring current. The CMe_2 group gave two singlets at δ 1.18 and 1.37, and the OCH_2 protons were observed as two mutually coupled doublets at δ 2.94 and 4.18. In addition, two singlets were observed at δ 4.68 and 6.41 due to the original alkyne protons; there is no sign of a signal for MeCN. The FAB mass spectrum showed an ion at m/z 704, corresponding to the di-insertion of $\text{PhC}\equiv\text{CH}$ with no coordination of MeCN.

Fortunately we were able to obtain suitable crystals of **7a** and have been able to determine its structure by X-ray crystallography (see Figure 5). The structure shows an eight-membered metallacycle formed by insertion of two molecules of $\text{PhC}\equiv\text{CH}$ into the M–C bond of **5a**. The

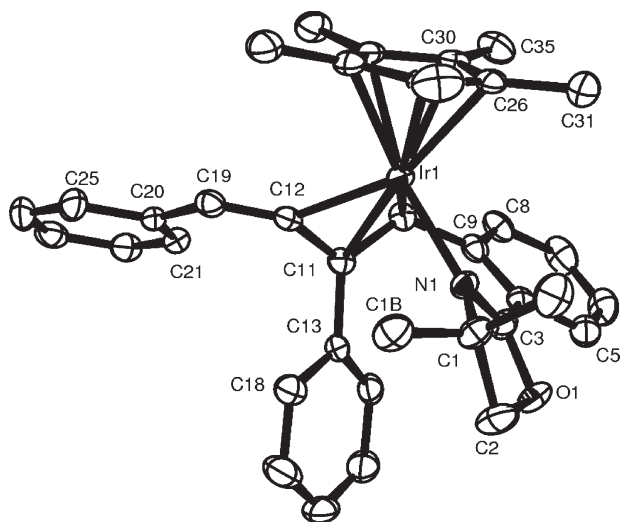


Figure 5. Molecular structure and atom-numbering scheme for the cation of **7a** with 50% displacement ellipsoids. All H atoms are omitted for clarity. Selected bond distances (Å) and angles (deg): Ir–N(1) 2.096(3), Ir–C(10) 2.150(4), Ir–C(11) 2.241(4), Ir–C(12) 2.093(4), Ir–C(26) 2.228(4), Ir–C(27) 2.250(4), Ir–C(28) 2.235(4), Ir–C(29) 2.167(4), Ir–C(30) 2.224(4), C(9)–C(10) 1.470(6), C(10)–C(11) 1.449(6), C(11)–C(12) 1.402(6), C(12)–C(19) 1.323(6), C(10)–Ir–N(1) 87.58(15).

organic fragment is bonded through the oxazoline nitrogen and has an η^3 -interaction with three of the alkyne carbon atoms; isomerization of the end alkyne unit has occurred to give a vinylidene. The η^3 -allyl is bonded asymmetrically with Ir–C(12) being the shortest bond (2.093(4) Å) and Ir–C(11) being the longest at 2.241(4) Å. The phenyl substituent [C(13)–C(18)] on the central carbon atom of the allyl is oriented anti with respect to the Cp* on Ir.

We have established that insertion of alkynes into the M–C bond of cyclometalated phenyl oxazoline complexes occurs under very mild conditions if the starting complexes have an easily substituted ligand such as MeCN. Many cyclopalladated complexes undergo insertion reactions with CO as well as with alkynes.³⁰ To our knowledge there is only one report of half-sandwich cyclometalated complexes with CO,³¹ and these do not undergo insertion; hence we have tested the reaction of **2a** with CO.

Carbon monoxide was bubbled through a solution of **2a** in CDCl₃. After 1.5 h the ¹H NMR spectrum showed complete conversion to a new product, **8a**. After recrystallization the ¹H NMR spectrum of **8a** shows no MeCN present, the CMe₂ group is observed as two singlets at δ 1.30 and 1.50, and the OCH₂ protons are observed as two mutually coupled doublets at δ 4.20 and 4.22. These observations are consistent with a chiral metal center and that, unlike **2a**, no epimerization occurs on the NMR time scale. The ¹³C{¹H} NMR spectrum shows the expected signals for the Cp* and oxazoline ligand with an additional signal at δ 165.52 assigned to a terminal CO. The FAB mass spectrum shows a molecular ion at m/z

530 and a fragment ion at m/z 502 [M – CO]⁺. The $\nu(\text{CO})$ absorption is observed at 2042 cm⁻¹ as expected for a terminal CO and similar to those (2030 and 2036 cm⁻¹) reported for analogous complexes.³¹ There was no evidence for any insertion product under these reaction conditions.

In conclusion, we have shown that both internal and terminal alkynes will insert into half-sandwich cyclometalated phenyl oxazoline complexes. In all cases if only one equivalent of alkyne is used, then monoinsertion products can be isolated. The insertion seems to favor the isomer with the more electron-withdrawing group next to the metal, but more studies are needed to confirm the generality of this. In no case does reductive elimination with concomitant C–N bond formation occur spontaneously, and we have not yet examined whether oxidizing agents can promote this transformation. The MeCN ligand of **2a** is also easily displaced by CO; however in this case no subsequent insertion is observed.

Experimental Section

The reactions described were carried out under nitrogen using dry solvents; however, once isolated as pure solids, the compounds can be handled in air. ¹H and ¹³C{¹H} NMR spectra were obtained using Bruker ARX250 or 300 MHz spectrometers, with CDCl₃ as solvent, unless otherwise stated. Chemical shifts were recorded in ppm (with tetramethylsilane as internal reference). FAB mass spectra were obtained on a Kratos concept mass spectrometer using NOBA as matrix. The electrospray (ES) mass spectra were recorded using a micromass Quattro LC mass spectrometer with dichloromethane or methanol as solvent. Infrared spectra were run as solids in a diamond ATR cell using a Perkin-Elmer Spectrum 1 instrument. Microanalyses were performed by the Elemental Analysis Service (University of North London). All starting materials were obtained from Aldrich, with the exception of [IrCl₂Cp*]₂,³² [RuCl₂(*p*-cymene)]₂,³³ complex **1a**, and oxazoline,³⁴ which were prepared by literature methods.

Preparation of 2a. A mixture of **1a** (70 mg, 0.13 mmol) and KPF₆ (55 mg, 0.30 mmol) in acetonitrile was stirred overnight. The mixture was filtered through Celite to remove excess KPF₆; the filtrate was evaporated to dryness and washed with hexane. The complex was recrystallized from dichloromethane/hexane, giving **2a** as a yellow solid (75 mg, 83.3%). Anal. Calcd for C₂₃H₃₀IrN₂OPF₆: C, 40.17, H, 4.40, N, 4.07. Found: C, 40.29, H, 4.37, N, 3.97. ¹H NMR: δ 1.47 (br, 6H, 2×Me), 1.80 (s, 15H, Cp*), 2.42 (br, 3H, NCMe), 4.58 (s, 2H, CH₂), 7.15 (dt, 1H, *J* 7.5, 1, H⁴), 7.33 (dt, 1H, *J* 7, 1.5, H⁵), 7.48 (dd, 1H, *J* 7.5, 1.5, H³), 7.75 (d, 1H, *J* 7.5, H⁶). ¹³C NMR: δ 3.45 (NCMe), 9.87 (C₅Me₅), 27.00 (Me), 28.27 (Me), 67.96 (CMe₂), 82.78 (OCH₂), 90.96 (C₅Me₅), 119.64 (NCMe), 123.74, 127.36, 133.38, 135.20 (C³, C⁴, C⁵, C⁶), 156.64 (NCO), 179.26 (C¹Ir). MS (FAB): m/z 502 [M – NCMe]⁺. IR: $\nu(\text{C}=\text{N})$ 1622 cm⁻¹.

Preparation of 2b. A mixture of NaOAc (34 mg, 0.41 mmol), [RuCl₂(*p*-cymene)]₂ (100 mg, 0.16 mmol), the oxazoline (57 mg, 0.33 mmol), and KPF₆ (120 mg, 0.65 mmol) was heated at 45 °C in acetonitrile for 3 h. The mixture was filtered through Celite, evaporated to dryness, and washed with ether to give **2b** as a green solid (180 mg, 92%). Anal. Calcd for C₂₃H₂₉N₂ORuPF₆: C, 46.39, H, 4.91, N, 4.70. Found: C, 46.23, H, 4.80, N, 4.62. ¹H NMR: δ 0.84 (d, 3H, *J* 7, CHMeMe'), 1.09 (d, 3H, *J* 7, CHMeMe'), 1.47 (s, 3H, oxaz-Me), 1.57 (s, 3H, oxaz-Me), 2.14 (s, 3H, Cy-Me), 2.21 (s, 3H, NCMe), 2.48 (sept, 1H, *J* 7, CyCHMeMe), 4.50 (s, 2H, NCH₂), 5.21 (d, 1H, *J* 6, Cy), 5.26

(30) For example see: (a) Thompson, J. M.; Heck, R. F. *J. Org. Chem.* **1975**, *40*, 2667. (b) Tollari, S.; Cenini, S.; Tunice, C.; Palmisano, G. *Inorg. Chim. Acta* **1998**, *272*, 18. (c) Tollari, S.; Demartin, F.; Cenini, S.; Palmisano, G.; Raimondi, P. *J. Organomet. Chem.* **1997**, *527*, 93. (d) Lindsell, W. E.; Palmer, D. D.; Preston, P. N.; Rosair, G. M.; Jones, R. V. H.; Whitton, A. J. *Organometallics* **2005**, *24*, 1119.

(31) Arita, S.; Koike, T.; Kayaki, Y.; Ikariya, T. *Organometallics* **2008**, *27*, 2795.

(32) White, C.; Yates, A.; Maitlis, P. M. *Inorg. Synth.* **1992**, *29*, 228.

(33) Bennett, M. A.; Smith, A. K. *J. Chem. Soc., Dalton Trans.* **1974**, 233.

(34) Denmark, S. E.; Nakajima, N.; Nicaise, O. J.-C.; Faucher, A.-M.; Edwards, J. P. *J. Org. Chem.* **1995**, *60*, 4884.

(d, 1H, *J* 6, Cy), 5.92 (d, 2H, *J* 6, Cy), 6.07 (d, 1H, *J* 6, Cy), 7.08 (dt, 1H, *J* 7.5, 1, H⁴), 7.29 (dt, 1H, *J* 7.5, 1.5 H⁵), 7.40 (dd, 1H, *J* 7.5, 1, H³), 8.03 (d, 1H, *J* 7.5, H⁶). ¹³C NMR: δ 3.54 (NCMe), 18.97 (Cy-MeC₆H₄), 21.35, 23.54 (Cy-CHMeMe), 27.65, 28.04 (oxz-MeMe') 31.28 (CyCHMeMe), 67.28 (CMe₂), 81.55, 82.24, 91.35, 91.37, (CH (C₆H₄Cy)), 81.95 (CH₂), 104.64, 105.92 (C (C₆H₄ Cy)), 124.03 (NCMe), 123.83, 126.99, 131.92, 139.72 (C³, C⁴, C⁵, C⁶), 173.12 (NCO), 175.92 (C¹Ru). MS (FAB): *m/z* (%) 410 [M]⁺, 451 [M - NCMe]⁺. IR: ν(C=N) 1622 cm⁻¹.

Preparation of 3a. PhC≡CPh (67 mg, 0.38 mmol) and KPF₆ (103 mg, 0.56 mmol) were added to a solution of **1a** (100 mg, 0.19 mmol) in acetonitrile; after stirring for 72 h, no insertion was observed by EMS. Other experiments (see above) show that at this stage **2a** was formed. The acetonitrile was replaced by dichloromethane, and the solution was stirred for 24 h and filtered through Celite to remove excess KPF₆. The filtrate was evaporated to dryness and then washed with hexane to give **3a** as a yellow solid (122 mg, 76%). Anal. Calcd for C₃₇H₄₀IrN₂OPF₆: C, 51.32; H, 4.66; N, 3.24. Found: C, 51.12; H, 4.53; N, 3.31. ¹H NMR: δ 1.31 (s, 3H, CMeMe'), 1.37 (s, 3H, CMeMe'), 1.41 (s, 15H, Cp*), 2.00 (s, 3H, NCMe), 4.27 (d, 1H, *J* 9, OCHH'), 4.58 (d, 1H, *J* 9, OCHH'), 6.30 (br, 1H, Ph), 6.74 (br m, 2H, Ph), 6.81 (br m, 2H, Ph), 6.99 (m, 5H, H⁶, Ph), 7.24 (m, 2H, H⁴, Ph), 7.31 (dt, 1H, *J* 7.5, 1.5, H⁵), 7.72 (dd, 1H *J* 7.5, 1, H³). ¹³C NMR: δ 2.35 (NCMe), 8.74 (C₅Me₅), 24.64, 27.57 (2×Me), 72.31 (CMeMe'), 81.50 (CH₂), 91.66 (C₅Me₅), 124.80 (NCMe), 124.17, 125.32, 125.95, 127.52, 128.12, 131.72, 132.40, 134.14 (Ar-H), 141.88 (C²), 146.3, 147.91 (C¹, C⁷), 151.38 (C, Ph of alkyne), 152.40 (C⁸), 169.16 (CNO). MS (FAB): *m/z* 679 [M - NCMe]⁺. IR: ν(C=N) 1624 cm⁻¹.

Preparation of 3b. PhC≡CPh (33 mg, 0.19 mmol) was added to solution of **2b** (100 mg, 0.17 mmol) in dichloromethane. After stirring for 24 h the solution was evaporated to dryness and then washed with hexane. The ¹H NMR spectrum suggested the compound was not pure, so it was washed through a short plug of silica (DCM/NCMe) to give **3b** as a pure complex as a green solid (66 mg, 51%). Anal. Calcd for C₃₇H₃₉RuN₂OPF₆: C, 57.43, H, 5.08, N, 3.62. Found: C, 55.81, H, 4.67, N, 3.29. ¹H NMR: δ 1.09 (s, 3H, oxz Me), 1.11 (d, 1H, *J* 7, CHMeMe'), 1.31 (d, 1H, *J* 7, CHMeMe'), 1.59 (s, 3H, oxz Me), 1.78 (s, 3H, NCMe), 2.27 (s, 3H, Me-Cy), 2.90 (sept, 1H, *J* 7, CHMeMe'), 4.34 (d, 1H, *J* 9, OCHH'), 4.35 (d, 1H, *J* 6, Cy), 4.47 (d, 1H, *J* 9, OCHH'), 4.54 (d, 1H, *J* 6, Cy), 5.10 (d, 1H, *J* 6, Cy), 5.65 (d, 1H, *J* 6, Cy), 6.18 (d, 1H, *J* 8, Ph), 6.73 (t, 1H, *J* 7.5, Ph), 6.83 (m, 3H, Ph), 6.96 (m, 3H, Ph), 7.14 (d, 1H, *J* 7.5, H⁶), 7.31 (m, 3H, H⁴, Ph), 7.38 (dt, 1H, *J* 7.5, 1.5, H⁵), 7.62 (dd, 1H, *J* 7.5, 1, H³). ¹³C NMR: δ 2.99 (NCMe), 19.57 (Me-Cy), 22.74, 24.45 (CHMeMe'), 25.44, 28.28 (2×Me), 31.61 (CH¹Pr), 71.08 (CMe₂), 81.57 (OCH₂), 80.32, 85.32, 88.09, 91.28 (CH(C₆H₄)), 109.46, 112.61 (C(C₆H₄)), 126.46 (NCMe), 124.32, 125.57, 126.25, 127.80, 128.49, 131.80, 132.02, 133.58, (Ar-H), 141.87 (C²), 145.92, 148.88 (C¹, C⁷), 151.54 (C, Ph of alkyne), 168.64 (C⁹), 171.46 (C⁸). MS (FAB): *m/z* 588 [M - NCMe]⁺. IR: ν(C=N) 1602 cm⁻¹.

Preparation of 4a. PhC≡CCO₂Et (21 mg, 0.12 mmol) was added to solution of **2a** (75 mg, 0.11 mmol) in dichloromethane; after stirring for 3 h, the solution was filtered through Celite, evaporated to dryness, and then washed with hexane. The ¹H NMR spectrum suggested the compound was not pure, so it was washed through a short plug of silica (DCM/NCMe) to give **4a** as a beige solid (66 mg, 51%). Anal. Calcd for C₃₄H₄₀IrN₂O₃PF₆: C, 47.38, H, 4.68, N, 3.25. Found: C, 47.25, H, 4.63, N, 3.16. ¹H NMR: δ 1.31 (s, 3H, CMeMe'), 1.38 (m, 3H, CO₂CH₂CH₃), 1.41 (s, 15H, Cp*), 1.46 (s, 3H, CMeMe'), 2.77 (s, 3H, NCMe), 3.79 (m, 2H, CO₂CH₂CH₃), 4.23 (d, 1H, *J* 9, OCHH'), 4.53 (d, 1H, *J* 9, OCHH'), 7.06 (m, 3H, Ph), 7.26 (m, 2H, H⁴, H⁶, Ph), 7.36 (m, 1H, H⁵), 7.68 (dd, 1H, *J* 7.5, 1, H³). ¹³C NMR: δ 4.12 (NCMe), 8.53 (C₅Me₅), 14.15 (CO₂CH₂CH₃), 24.63, 27.24 (2×Me), 59.48 (CO₂CH₂CH₃), 72.79 (CMeMe'),

81.65 (OCH₂), 91.93 (C₅Me₅), 124.56 (NCMe), 126.67, 127.05, 128.22, 129.96, 131.92, 132.52, 133.61 (Ar-H), 142.64 (C⁸), 144.69 (C¹), 168.71 (CNO) (other quaternary carbons are not seen). MS (FAB): *m/z* 676 [M - NCMe]⁺. IR: ν(C=N): 1624 cm⁻¹; ν(C=O) 1695 cm⁻¹.

Preparation of 5a. Phenylacetylene (11 mg, 0.11 mmol) was added to solution of **2a** (73 mg, 0.11 mmol) in dichloromethane, and the mixture was stirred for 1 h. The mixture was then filtered through Celite to remove excess KPF₆, and the filtrate was evaporated to dryness and washed with hexane to give **5a** as a pale yellow solid (72 mg, 86%). Anal. Calcd for C₃₁H₃₆IrN₂OPF₆: C, 47.14, H, 4.59, N, 3.55. Found: C, 47.28, H, 4.37, N, 3.47. ¹H NMR: δ 1.14 (s, 3H, CMeMe'), 1.29 (s, 3H, CMeMe'), 1.34 (s, 15H, Cp*), 1.99 (s, 3H, NCMe), 4.11 (d, 1H, *J* 9, OCHH'), 4.42 (d, 1H, *J* 9, OCHH'), 6.97 (m, 2H, Ph), 7.06 (m, 2H, H⁷, Ph), 7.20 (m, 4H, H⁴, H⁶, Ph), 7.41 (dt, 1H, *J* 7.5, 1.5, H⁵), 7.63 (dt, 1H, *J* 8, 1.5, H³). ¹³C NMR: δ 2.67 (NCMe), 8.93 (C₅Me₅), 24.89, 27.33 (2×Me), 72.66 (CMeMe'), 81.08 (CH₂), 91.55 (C₅Me₅), 121.84 (NCMe), 122.97 (C, Ph), 125.82, 127.02, 125.82, 132.07, 132.11, 133.02 (Ar-H), 132.11 (C⁷), 143.63 (C¹), 152.59 (C, Ph of alkyne), 155.68 (C⁸), 169.00 (CNO). MS (FAB): *m/z* 602 [M - NCMe]⁺. IR: ν(C=N) 1527 cm⁻¹.

Preparation of 5b. PhC≡CH (33 mg, 0.33 mmol) was added to solution of **2b** (194 mg, 0.33 mmol) in dichloromethane; after stirring overnight, the mixture was filtered through Celite, evaporated to dryness, and then washed with hexane. The ¹H NMR spectrum suggested the compound was not pure, so it was washed through a short plug of silica (DCM/NCMe) to give **5b** as an orange solid (120 mg, 53%). Anal. Calcd for C₃₁H₃₅RuN₂OPF₆: C, 53.37, H, 5.06, N, 4.02. Found: C, 53.47, H, 5.01, N, 3.95. ¹H NMR: δ 1.00 (s, 3H, oxz Me), 1.18 (d, 1H, *J* 7, CHMeMe'), 1.21 (d, 1H, *J* 7, CHMeMe'), 1.58 (s, 3H, oxz Me), 1.85 (s, 3H, NCMe), 2.06 (s, 3H, Me-Cy), 2.71 (sept, 1H, *J* 7, CHMeMe'), 4.32 (d, 1H, *J* 9, OCHH'), 4.35 (d, 1H, *J* 9, OCHH'), 4.39 (dd, 1H, *J* 6, 1, Cy), 5.03 (dd, 1H, *J* 6, 1, Cy), 5.35 (dd, 1H, *J* 6, 1, Cy), 5.41 (dd, 1H, *J* 6, 1, Cy), 7.12 (m, 4H, H⁷, Ph), 7.29 (m, 4H, H⁴, H⁶, Ph), 7.50 (dt, 1H, *J* 7.5, 1.5, H⁵), 7.68 (d, 1H, *J* 7.5, H³). ¹³C NMR: δ 3.05 (NCMe), 19.43 (Me-Cy), 22.73, 23.69 (CHMeMe'), 25.28, 27.63 (2×Me), 31.37 (CH¹Pr), 71.01 (CMe₂), 80.58 (CH₂), 82.00, 84.76, 87.84, 88.68 (CH(C₆H₄)), 108.07, 113.97 (C(C₆H₄)), 124.01 (NCMe), 125.60, 125.90, 127.28, 128.05, 130.66, 131.43, 132.08 (Ar-H), 132.32 (C⁷), 143.72 (C¹), 152.48 (C, Ph of alkyne), 168.57 (CNO), 176.01 (C⁸). MS (FAB): *m/z* 512 [M - NCMe]⁺. IR: ν(C=N) 1635 cm⁻¹.

Preparation of 6a. EtO₂CC≡CH (21 mg, 0.22 mmol) was added to solution of **2a** (75 mg, 0.11 mmol) in dichloromethane. After stirring for 3 h, the mixture was filtered through Celite, evaporated to dryness, and then washed with hexane to give **6a** as a pale yellow solid (70 mg, 82%). Anal. Calcd for C₂₈H₃₆IrN₂O₃PF₆: C, 42.80, H, 4.62, N, 3.57. Found: C, 42.70, H, 4.51, N, 3.56. ¹H NMR: δ 1.22 (s, 3H, CMeMe'), 1.27 (m, 3H, CO₂CH₂CH₃), 1.30 (s, 15H, Cp*), 1.37 (s, 3H, CMeMe'), 2.71 (s, 3H, NCMe), 4.11 (m, 3H, CO₂CH₂CH₃, overlap, d, 1H, *J* 9, OCHH'), 4.38 (d, 1H, *J* 9, OCHH'), 7.22 (m, 2H, H⁴, H⁶), 7.45 (dt, 1H, *J* 7.5, 1.5, H⁵), 7.48 (s, 1H, H⁷), 7.62 (d, 1H, *J* 7.5, H³). ¹³C NMR: δ 3.93 (NCMe), 8.61 (C₅Me₅), 14.84 (CO₂CH₂CH₃), 24.81, 27.37 (2×Me), 60.52 (CO₂CH₂CH₃), 72.99 (CMeMe'), 81.14 (OCH₂), 91.67 (C₅Me₅), 123.25 (NCMe), 126.95, 131.82, 132.43, 133.09 (C³, C⁴, C⁵, C⁶), 136.60 (C⁷), 141.65, 144.01 (C¹, C⁸), 168.64 (CNO), 174.70 (CO₂). MS (FAB): *m/z* 600 [M - NCMe]⁺. IR: ν(C=N) 1622 cm⁻¹; ν(C=O) 1682 cm⁻¹.

Preparation of 7a. PhC≡CH (21.6 mg, 0.22 mmol) was added to solution of **2a** (73 mg, 0.11 mmol) in dichloromethane; after stirring for 2 h, the mixture was filtered through Celite, evaporated to dryness, and then washed with hexane to give **7a** as a brown solid (80 mg, 89%). Anal. Calcd for C₃₇H₃₉IrNOPF₆: C, 52.23, H, 4.62, N, 1.65. Found: C, 52.23, H, 4.54, N, 1.64. ¹H NMR: δ 1.18 (s, 3H, CMeMe'), 1.37 (s, 3H, CMeMe'), 1.76

Table 1. Crystallographic Data for 2a, 3b, 5a, 5b, and 7a

	2a	3b	5a	5b	7a
empirical formula	C ₂₃ H ₃₀ F ₆ IrN ₂ OP	C ₃₇ H ₃₇ F ₆ N ₂ OPRu	C ₃₁ H ₃₆ F ₆ IrN ₂ OP	C ₃₁ H ₃₅ F ₆ N ₂ OPRu	C ₇₅ H ₈₀ Cl ₂ F ₁₂ Ir ₂ N ₂ O ₂ P ₂
fw	687.66	771.73	789.79	697.65	1786.69
temperature/K	150(2)	150(2)	150(2)	150(2)	150(2)
cryst syst	monoclinic	triclinic	monoclinic	monoclinic	triclinic
space group	<i>C2/c</i>	<i>P</i> $\bar{1}$	<i>P2(1)/c</i>	<i>P2(1)/c</i>	<i>P</i> $\bar{1}$
<i>a</i> /Å	25.528(4)	9.4592(12)	13.9443(10)	15.3684(8)	10.2780(12)
<i>b</i> /Å	12.890(2)	10.6699(13)	12.4836(8)	8.6735(5)	10.6585(13)
<i>c</i> /Å	15.351(3)	19.855(3)	18.8176(13)	22.3405(12)	16.300(2)
α /deg	90	93.500(2)	90	90	90.631(2)
β /deg	95.196(3)	103.563(2)	106.414(1)	96.764(1)	97.335(2)
γ /deg	90	114.285(2)	90	90	101.336(2)
<i>U</i> /Å ³	5030.4(15)	1747.4(4)	3142.2(4)	2957.2(3)	1735.3(4)
<i>Z</i>	8	2	4	4	1
density (calcd)/Mg/m ³	1.816	1.467	1.670	1.567	1.710
abs coeff/mm ⁻¹	5.435	0.558	4.363	0.650	4.034
<i>F</i> (000)	2688	788	1560	1424	886
cryst size/mm	0.22 × 0.20 × 0.09	0.29 × 0.21 × 0.18	0.34 × 0.13 × 0.07	0.29 × 0.21 × 0.18	0.21 × 0.11 × 0.09
theta range/deg	1.60 to 26.00	2.13 to 25.00	1.52 to 26.00	1.33 to 25.00	1.26 to 27.00
index ranges	−31 ≤ <i>h</i> ≤ 31, −15 ≤ <i>k</i> ≤ 15, −18 ≤ <i>l</i> ≤ 18	−11 ≤ <i>h</i> ≤ 11, −12 ≤ <i>k</i> ≤ 12, −23 ≤ <i>l</i> ≤ 23	−17 ≤ <i>h</i> ≤ 17, −15 ≤ <i>k</i> ≤ 15, −23 ≤ <i>l</i> ≤ 23	−18 ≤ <i>h</i> ≤ 18, −10 ≤ <i>k</i> ≤ 10, −26 ≤ <i>l</i> ≤ 26	−13 ≤ <i>h</i> ≤ 13, −13 ≤ <i>k</i> ≤ 13, −20 ≤ <i>l</i> ≤ 20
reflns collected	19 090	12 602	23 528	20 816	14 726
indep reflns (<i>R</i> _{int})	4938 [<i>R</i> (int) = 0.0335]	6076 [<i>R</i> (int) = 0.0310]	6165 [<i>R</i> (int) = 0.0787]	5210 [<i>R</i> (int) = 0.0896]	7434 [<i>R</i> (int) = 0.0305]
data/restraints/params	4938/0/315	6076/0/458	6165/72/440	5210/0/431	7434/0/449
goodness-of-fit, <i>F</i> ²	1.057	1.044	0.955	1.056	0.972
final <i>R</i> indices [<i>I</i> > 2σ(<i>I</i>)]	<i>R</i> 1 = 0.0240, w <i>R</i> 2 = 0.0648	<i>R</i> 1 = 0.0524, w <i>R</i> 2 = 0.1352	<i>R</i> 1 = 0.0420, w <i>R</i> 2 = 0.0884	<i>R</i> 1 = 0.0446, w <i>R</i> 2 = 0.1205	<i>R</i> 1 = 0.0345, w <i>R</i> 2 = 0.0694
<i>R</i> indices (all data)	<i>R</i> 1 = 0.0271, w <i>R</i> 2 = 0.0659	<i>R</i> 1 = 0.0598, w <i>R</i> 2 = 0.1408	<i>R</i> 1 = 0.0558, w <i>R</i> 2 = 0.0936	<i>R</i> 1 = 0.0471, w <i>R</i> 2 = 0.1229	<i>R</i> 1 = 0.0400, w <i>R</i> 2 = 0.0713
largest diff peak and hole/e Å ⁻³	1.549 and −1.662	1.199 and −0.730	3.595 and −0.827	1.255 and −1.132	1.882 and −1.679

(s, 15H, Cp*), 2.94 (d, 1H, *J* 9, OCHH'), 4.18 (d, 1H, *J* 9, OCHH'), 4.68 (s, 1H, H⁷), 6.41 (s, 1H, H¹⁰), 7.02 (m, 3H, Ph), 7.13 (m, 3H, Ph), 7.34 (m, 2H, Ph), 7.40 (dt, 1H, *J* 6.5, 1.5, H⁴), 7.50 (m, 2H, Ph), 7.55 (dd, 1H, *J* 7, 1, H⁶), 7.77 (dt, 1H, *J* 7, 1.5, H⁵), 7.83 (dd, 1H, *J* 7.5, 1, H³). ¹³C NMR: δ 9.50 (C₅Me₅), 25.99, 27.66 (2×Me), 48.58 (C⁷), 71.01 (CMeMe'), 80.44 (OCH₂), 95.99 (C₅Me₅), 104.92 (C⁹), 119.84 (C¹⁰), 127.37, 127.47, 127.90, 128.51, 128.69, 131.65, 132.32, 133.64 (Ar-H), 123.98, 125.38 (C, Ph), 133.75, 138.24 (C¹, C⁸), 152.61 (C), 165.33 (CNO). MS (FAB): *m/z* 704 [M]⁺. IR: ν(C=N) 1604 cm⁻¹.

Preparation of 8a. CO was bubbled through a solution of **2a** (42 mg, 0.62 mmol) in CDCl₃ for 1.5 h. The solution was evaporated to dryness and was recrystallized from dichloromethane/hexane to give **8a** as a yellow precipitate (38 mg, 92.3.3%). Anal. Calcd for C₂₂H₂₇IrN₂O₂PF₆: C, 39.17, H, 4.03, N, 2.08. Found: C, 39.05, H, 3.96, N, 1.97. ¹H NMR: δ 1.30 (s, 3H, Me), 1.50 (s, 3H, Me), 2.00 (s, 15H, Cp*), 4.20 (d, 1H, *J* 5, CHH') 4.22 (d, 1H, *J* 5, CHH'), 7.30 (dt, 1H, *J* 7.5, 1, H⁴), 7.43 (dt, 1H, *J* 7, 1.5, H⁵), 7.63 (m, 2H, H³, H⁶). ¹³C NMR: δ 10.05 (C₅Me₅), 27.05 (Me), 27.85 (Me), 69.20 (CMe₂), 81.99 (OCH₂), 102.17 (C₅Me₅), 126.01, 129.12, 134.42, 136.27 (C³, C⁴, C⁵, C⁶), 144.76 (C²), 165.52 (CO), 180.44 (C¹Ir). MS (FAB): *m/z* 530 [M]⁺, 502 [M - CO]⁺. IR: ν(C=O) 2042 cm⁻¹, ν(C=N) 1614 cm⁻¹.

X-ray Crystal Structure Determinations. Details of the structure determinations of crystals of **2a**, **3b**, **5a**, **5b**, and **7a** are given in Table 1. Data were collected on a Bruker Apex 2000 CCD diffractometer using graphite-monochromated Mo Kα radiation, λ = 0.7107 Å at 150 K. The data were corrected for Lorentz and polarization effects, and empirical absorption corrections (SADABS).³⁵ were applied in all cases. The structures were solved by Patterson methods and refined by full-matrix least-squares on *F*² using the program SHELXTL.³⁶ All hydrogen atoms bonded to carbon were included in calculated positions (C–H = 0.96 Å) using a riding model. All non-hydrogen atoms were refined with anisotropic displacement parameters without positional restraints. Figures were drawn using the program ORTEP.³⁷

Atomic coordinates, bond lengths and angles, and thermal parameters have been deposited at the Cambridge Crystallographic Data Centre, CCDC Nos. 758499–758503.

Acknowledgment. We thank the Saudi Arabian government (O.A.-D.) for a studentship and Johnson Matthey for a loan of iridium trichloride and ruthenium trichloride.

Supporting Information Available: This material is available free of charge via the Internet at <http://pubs.acs.org>.

(35) SADABS, Version 6.02; Bruker Inc.: Madison, WI, 1998–2000.

(36) SHELXTL, Version 6.10; Bruker Inc.: Madison, WI, 1998–2000.

(37) Farrugia, L. J. *J. Appl. Crystallogr.* **1997**, *30*, 565.